29th Congress of the International Council of the Aeronautical Sciences
St. Petersburg, Russia; September 7-12, 2014

INTERFERENCE BETWEEN BODIES IN HYPERSONIC RAREFIED-GAS FLOWS

Vladimir V. Riabov
Rivier University, Nashua, New Hampshire 03060, USA

Keywords: *hypersonic rarefied-gas flows; direct simulation Monte-Carlo method; flow interference; simple-shape bodies, toroidal balloon*

Abstract

Hypersonic flows near two side-by-side plates and cylinders, toroidal balloon, plate and cylinder over a plane surface, and a plate behind a cylinder in argon and nitrogen have been studied numerically using the direct simulation Monte-Carlo technique (DSMC) under the transitional flow regime conditions at Knudsen numbers $0.004 \le Kn_\infty \le 10$. Strong influences of the geometrical factor (the ratio of a distance between bodies to a body length) and the Knudsen number on the flow structure about the bodies (the shape of shock waves, the configuration of subsonic flow zones) and on skin friction, pressure distribution, lift and drag have been found.

1 Introduction

Experimental and numerical studies [1-4] of aerodynamics of simple shape bodies have provided valuable information related to physics of hypersonic flows about spacecraft elements and testing devices. Numerous results had been found in the cases of plates, wedges, cones, disks, spheres, torus, and cylinders (see Refs. 1-7). The interference effect for flat strips and cylinder grids was experimentally studied by Coudeville *et al* [8] for transition rarefied-gas flows. Supersonic, subsonic, and pressure-driven, low-speed flows in two-dimensional microchannels of varying aspect ratios, $20 \ge L/2H \ge 2.5$, were studied with the DSMC technique by Mavriplis *et al* [9] and Oh *et al* [10] for a range of continuum to transitional rarefied-gas flow regimes. The results [9,10] were in qualitative agreement with other computational and experimental results for longer microchannels. Near the continuum limit, they show the same trends as classical theories, such as Fanno-Rayleigh flow and boundary-layer interaction with shocks [9].

In the present study, the hypersonic rarefied-gas flow about two side-by-side plates of varying small aspect ratios, $2 \ge L/2H \ge 0.4$, has been studied at Knudsen numbers $Kn_{\infty,L}$ from 0.024 to 1.8. The flow pattern for such a configuration has not been discussed in the research literature. Numerical results have been obtained using the direct simulation Monte Carlo (DSMC) technique [2] and the computer code [11] developed by Graeme Bird. Several features of the flow are unique. For example, if the distance between the plates, $2H$, is significantly larger the plate length L, than the flow can be approximated by a stream between two isolated plates [2-6]. At $H \le 0.25L$, the rarefied gas flow has some features of a stream near a bluff body [12]. In the first case, two oblique shock waves interact in the vicinity of the symmetry plane generating the normal shock wave and the Mach reflected waves far behind the bodies. In the second case, the front shock wave would be normal and the pressure and skin-friction distributions along the upper and bottom surfaces would be difficult to predict. At $H \le 0.5L$, the flow pattern and shock-wave shapes are very complex. Therefore, simple approximations should not be used to define the aerodynamics of side-by-side bodies.

Flow about two side-by-side cylinders, their aerodynamic characteristics, and interference between cylinder and a plane

surface have also been studied under the conditions of a hypersonic rarefied-gas stream at Knudsen numbers $Kn_{\infty,R}$ from 0.0167 to 10 and a range of geometrical factors ($6R \geq H \geq 2R$). For $3R \geq H$, the repulsive lift force has been found to become significant with a lift-drag ratio of 0.35. Blevins [12] previously analyzed the continuum streams.

Finally, the rarefied-nitrogen flow about a blunt plate located in the wake of a cylindrical wire has been numerically studied. Hayes and Probstein [13], Oguchi [14], and Allègre and Bisch [15] showed that the skin friction and pressure coefficients are maximal near the leading edge of the plate. Bisch [16] offered a unique experimental technique of the friction reduction by adding a wire-shaped "fore-leading edge" in front of the plate. The identical study of continuum flow regimes was made by Yegorov *et al* [17]. It was found that the induced wake flow in front of the plate reduced the strength of the shock wave and resulted in reducing the plate drag and friction.

2. DSMC method

The DSMC method [2] and the two-dimensional DS2G code [11] have been used in this study as a numerical simulation technique for low-density hypersonic gas flows. Molecular collisions in argon and nitrogen are modeled using the variable hard sphere molecular model [2]. The gas-surface interactions are assumed to be fully diffusive with full moment and energy accommodation, and the wall temperature is equal to the stagnation temperature.

Code validation was established [4,18] by comparing numerical results with experimental data [3,4] related to simple-shape bodies. As an example, the comparison of the DSMC recent numerical results with experimental data [5] in air is shown in Fig. 1 for a wide range of Knudsen numbers from 0.02 to 3.2 and flow parameters: $M_\infty = 10$, $\gamma = 1.4$, and $t_w = 1$. The error of experimental data [5] (see error bars in Fig. 1) was estimated as 8-12% at different flow regimes (see Ref. 5 and the bibliography in Ref. 4). The numerical results correlate well with experimental data at $0.02 < Kn_{\infty L} < 1$ and approach the free-molecular limit [20] at $Kn_{\infty,L} > 3$.

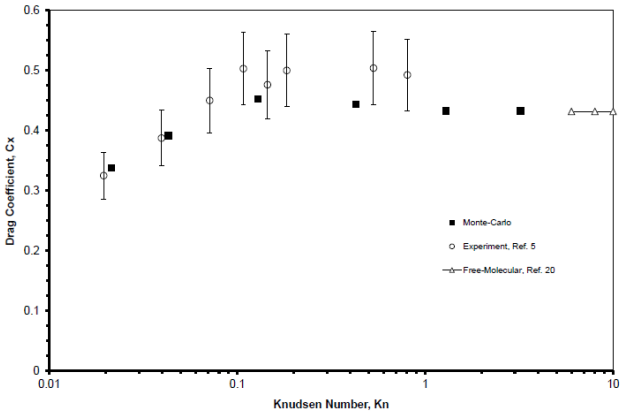

Fig. 1. Total drag coefficient of the plate vs Knudsen number $Kn_{\infty,L}$ in air at $M_\infty = 10$.

The methodology from Refs. 2, 9 and 11 has been applied in computations. The cases that had been considered by Mavriplis *et al* [9] for airflows in near-continuum, transitional and near-free-molecular regimes were reproduced in this study.

Table 1. Drag coefficient of a single plate in airflow at $Kn_{\infty,L} = 0.13$, $M_\infty = 10$, $\gamma = 1.4$, $t_w = 1$, and different numerical parameters

Number of cells	Number of molecules per cell	Drag coefficient	Time of calculation
12,700	11	0.4524	12 h. 28 min.
12,700	22	0.4523	21 h. 03 min.
49,400	11	0.4525	62 h. 06 min.
203,200	11	0.4526	187 h. 11 min.

The mesh size and the number of molecules per cell were varied until independence of the flow profiles and aerodynamic characteristics from these parameters was achieved for each case [18]. The mesh size and the number of molecules per cell were varied until independence of the flow profiles and aerodynamic characteristics from these parameters was achieved for each case. Table 1 shows the DSMC results for the drag coefficient of the plate C_x in the airflow at $Kn_{\infty L} = 0.13$, $M_\infty = 10$, $\gamma = 1.4$, $t_w = 1$, and different computational parameters. The uniform grid has covered the symmetrical flow area 0.024 m × 0.021 m near the plate 0.01 m × 0.001 m. The

location of the external boundary with the upstream flow conditions is at 0.01 m from the leading edge of the plate. It has been found that the numerical solutions for C_x are independent of the numerical parameters (see Table 1).

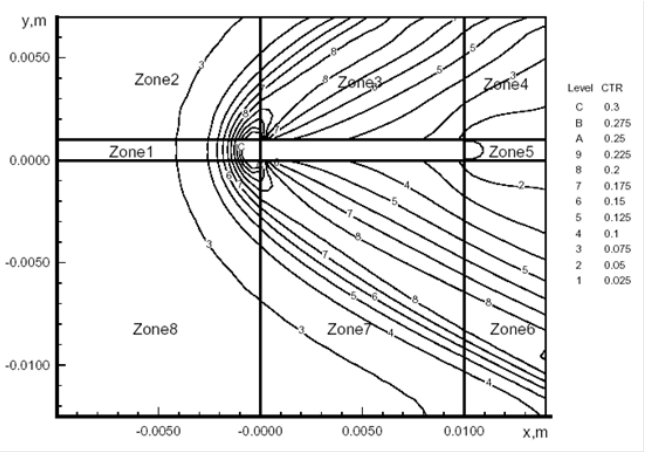

Fig. 2 CTR [11] of the time step to the local mean collision time in argon flow about a side-by-side plate at $Kn_{\infty,L}$ = 0.024 and H = 1.25L.

The similar mesh parameters have been used in the case of two side-by-side plates. As an example, for calculations at H/L = 1.25, the total number of cells near a plate (a half-space of the flow segment between side-by-side plates) is 12,700 in eight zones (see Fig. 2), the argon molecules are distributed evenly, and a total number of 139,720 molecules corresponds to an average 11 molecules per cell. The location of the external boundary with the upstream flow conditions varies from 0.75L to 1.5L. Following the recommendations of Refs. 2 and 11, acceptable results are obtained for an average of at least ten molecules per cell in the most critical region of the flow. The error was pronounced when this number falls below five. The cell geometry has been chosen to minimize the changes in the macroscopic properties (pressure and density) across the individual cell [11]. In all cases the usual criterion [2] for the time step Δt_m has been realized, $1\times10^{-8} \le \Delta t_m \le 1\times10^{-6}$ s. Under these conditions, aerodynamic coefficients and gas-dynamic parameters have become insensitive to the time step. The ratios of the mean separation between collision partners to the local mean free path and the collision time ratio (CTR) [11] of the time step to the local mean collision time have been well under unity over the flowfield (see Fig. 2).

The total number of non-uniform cells [19] near a cylinder (a half-space of the flow segment between side-by-side plates for calculations at H/R = 3) is 2100, and 32,200 molecules are distributed evenly (an average 15 molecules per cell). The location of the external boundary varies from 2.5R to 4.5R.

In all cases the criterion for the time step Δt_m (recommended in Ref. 2) has been realized, $1\times10^{-8} \le \Delta t_m \le 1\times10^{-6}$ s. Under these conditions, aerodynamic coefficients and gas-dynamic parameters have become insensitive to the time step. The ratios of the mean separation between collision partners to the local mean free path and the ratio of the time step to the local mean collision time have been well under unity over the flowfield [18,19].

The DS2G program employed time averaging for steady flows [11]. About 200,000 samples have been studied in the considered cases. The computed results have been stored to the TECPLOT® files that have been further analyzed to study whether the DSMC numerical criteria [2] are met. Calculations were carried out on a personal computer with a Pentium® III 850-MHz processor. The computing time of each variant was estimated to be approximately 12 - 60 h.

3. Interference of two side-by-side plates

The flow pattern over two side-by-side plates is sensitive to the major geometrical similarity parameter, H/L. The influence of this factor on the stream structure has been studied for hypersonic flow of argon at M_∞ = 10 and $Kn_{\infty L}$ = 0.024. The flow pattern and shock-wave shapes are significantly different for large and small geometric ratios [21].

At H/L = 1.0, a strong oblique shock wave can be observed near the plate (see Fig. 3a). Two oblique shock waves interfere near the symmetry plane. The subsonic and supersonic areas (at M ≤ 2.5) of the flow near the plates are symmetrical, which indicates that there is no lift force acting on the plates for the specified conditions. At H/L = 0.5, the flow near a plate

becomes significantly asymmetrical, the disturbances interact in the vicinity of the symmetry plane, creating the Mach normal shock wave and a wide subsonic area, which occupies the whole "throat" area between two side-by-side plates (see Fig. 3b).

(a)

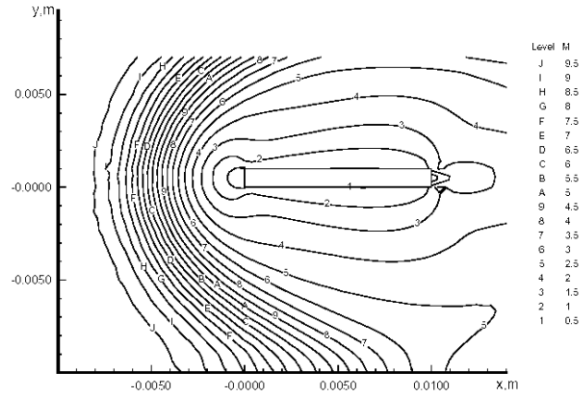

(b)

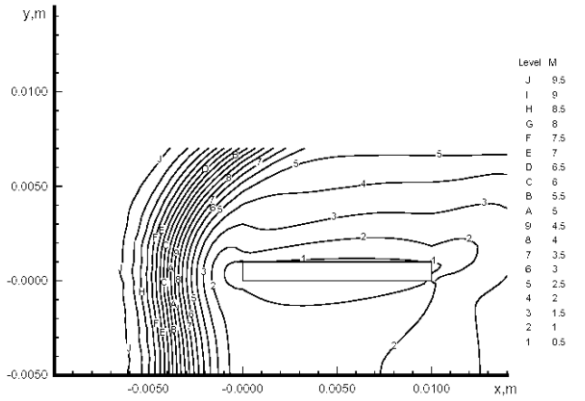

Fig. 3. Mach number contours in argon flow about a side-by-side plate at $Kn_{\infty,L}$ = 0.024 and various H/L-ratios: (a) $H = L$ and (b) $H = 0.5L$.

The latter effect plays a fundamental role in the redistribution of pressure and skin friction along the plate surface (Figs. 4a and 4b, respectively). This phenomenon produces significant repulsive lift force. A non-monotonous dependency of lift and drag from values of the Knudsen number has been found for various geometric factors (see Fig. 5). The drag approaches the free-molecular limit [20] at $Kn_{\infty,L} > 2$.

The rarefaction effects on the lift force are significant at all considered values of the geometrical factor ($1.25 \geq H/L \geq 0.25$). At small factors, the repulsive lift force on side-by-side plates becomes significant with the lift-drag ratio of 1.6 in near-continuum flow regime and essentially reduces (up to 0.4) in the near-free-molecular flow.

(a)

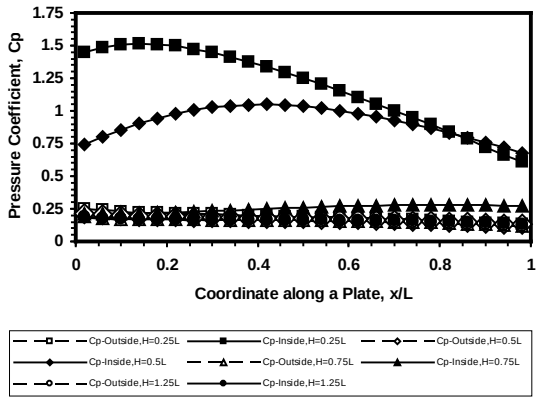

(b)

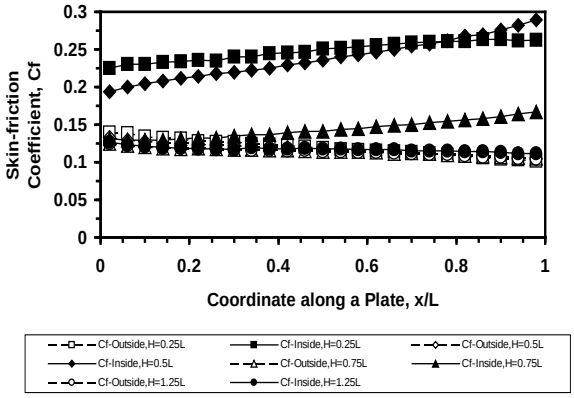

Fig. 4. Pressure and skin-friction coefficients along the side-by-side plate at $Kn_{\infty,L}$ = 0.024 at M_∞ = 10: (a) pressure coefficient and (b) skin-friction coefficient.

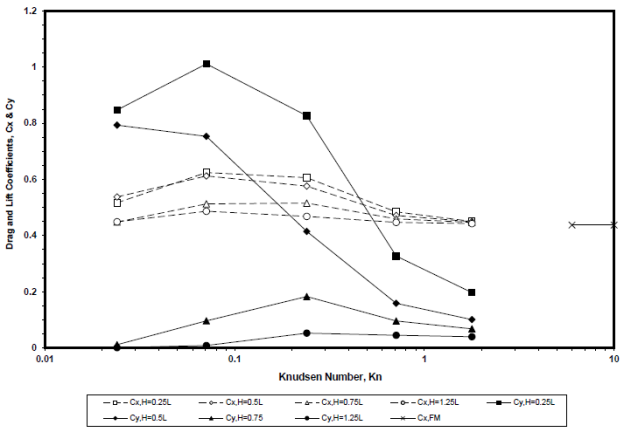

Fig. 5. Total drag and lift coefficients of the side-by-side plates vs. Knudsen number $Kn_{\infty,L}$ at M_∞ = 10.

4. Aerodynamics of two side-by-side cylinders

The flow pattern over two side-by-side cylinders is also sensitive to the major geometrical similarity parameter, H/R (see Figs. 6a and 6b). The influence of this parameter on the flow structure has been studied for hypersonic flow of argon at M_∞ = 10 and $Kn_{\infty,R}$ = 0.1. At the small ratio parameters, $H/R \le 2$, the front shock-wave shape becomes normal (see Fig. 6b), and front stagnation points (180°) relocate from the cylinder front zone towards the "throat" area (see Figs. 7a and 7b). This phenomenon [4,21] effects the drag, pressure and skin-friction distributions along a cylinder and produces significant repulsive lift force (see Fig. 8) with C_y/C_x = 0.35. The geometrical factor becomes insignificant on the drag both under continuum flow regime conditions and in free-molecule flow at $H/R \ge 4$.

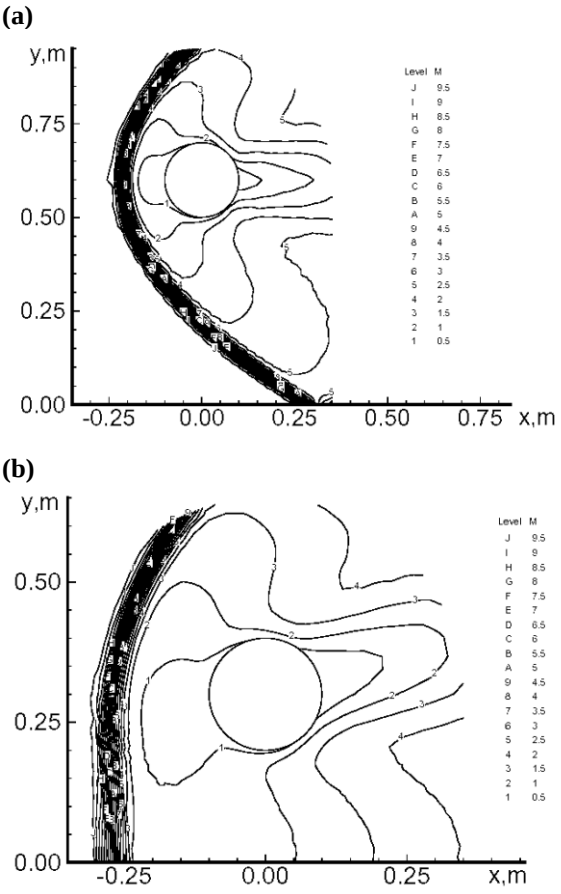

Fig. 6. Mach number contours in argon flow about a side-by-side cylinder at $Kn_{\infty,R}$ =0.1 and various H/R-ratios: (a) H=6R and (b) H=2R.

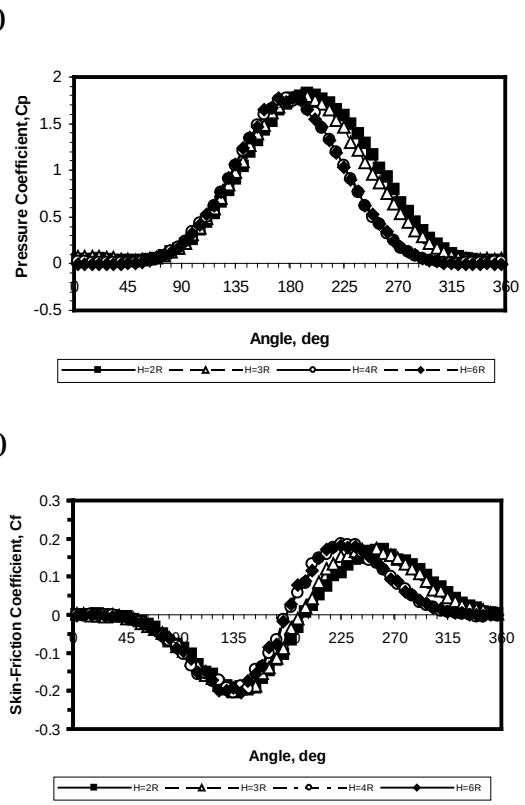

Fig. 7. Pressure and skin-friction coefficients along the side-by-side cylinder at $Kn_{\infty,R}$ = 0.1: (a) pressure coefficient and (b) skin-friction coefficient.

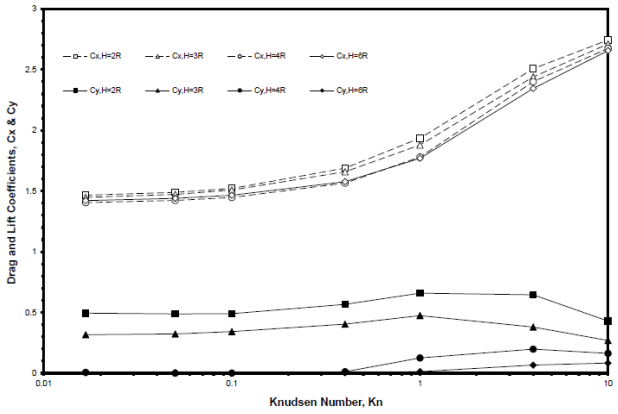

Fig. 8. Total drag and lift coefficients of the side-by-side cylinder vs. Knudsen number $Kn_{\infty,R}$ at M_∞ = 10.

5. Flow over a toroidal ballute

Aerocapture with large inflatable decelerators known as toroidal ballutes [22] is currently viewed as the most promising technology for a number of NASA's future robotic missions to Venus, Saturn, Titan, and Neptune [23-25]. In the present study, the hypersonic rarefied-gas flows about a torus and ballute model have been

studied. The flow pattern in argon was discussed in Ref 7.

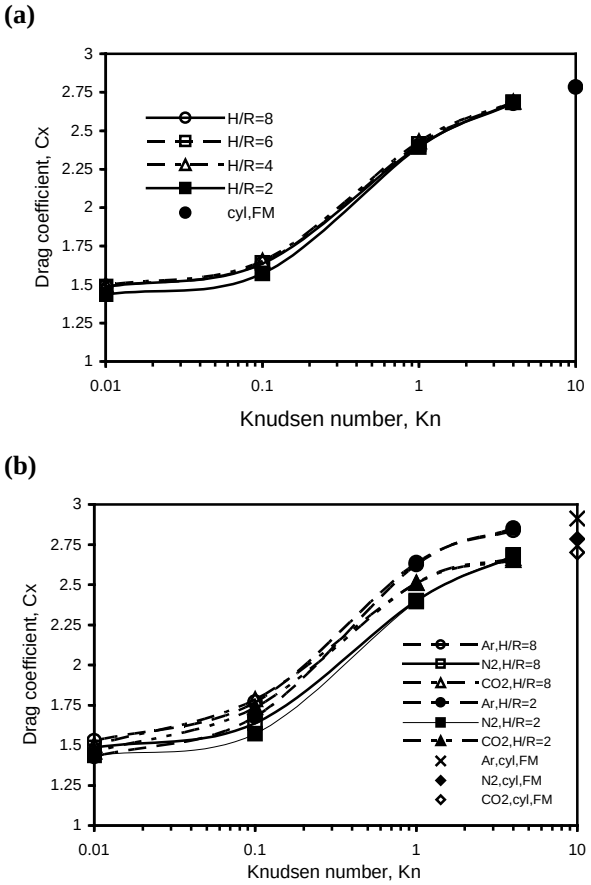

Fig. 9. Drag coefficient C_x of a torus vs Knudsen number $Kn_{\infty,D}$ at M_∞ = 10 and various geometrical factors H/R: (a) in nitrogen flows and (b) in flows of argon, nitrogen, and carbon dioxide.

Several features of the flow are unique. For example, if the distance between the axis of symmetry and the torus disk center H is significantly larger the torus radius R, then the flow can be approximated by a stream between two side-by-side cylinders [12,19,21]. At $H = R$, the rarefied gas flow has some features of a stream near a bluff disk [4,12]. In the first case, two conical shock waves would focus and interact in the vicinity of the symmetry axis generating the normal shock wave and the conical reflected waves. The stagnation points would be near the front points of the torus disks. In the second case, the front shock wave would be normal and the location of stagnation points would be difficult to predict. At $H > R$, the flow pattern and shock-wave shapes are very complex. As a result, simple approximation techniques would not be applied in torus aerothermodynamics.

In the present study, flows about a torus [21,28] and its aerodynamic characteristics have been investigated under the conditions of a hypersonic rarefied-gas stream of nitrogen, argon, dissociating oxygen, and carbon dioxide at $8R \geq H \geq 2R$ and the Knudsen number $Kn_{\infty,D}$ from 0.01 to 10.

The rarefaction factor, which can be characterized by the Knudsen number $Kn_{\infty,D}$, plays an important role in the flow structure [2,7] as well as in aerodynamics [4]. Under continuum flow conditions ($Kn_{\infty,D}$ = 0.01), the flow structure has the same features as were discussed above. In transitional flow regime, at $Kn_{\infty,D}$ = 1, the flow pattern is different [21,28]. The reflection waves have different shapes, because of the rarefaction effects in the conic and normal shock waves. At a small outer torus radius, H/R = 2, the skin-friction coefficient distribution along the torus surface becomes sensitive to the rarefaction parameter $Kn_{\infty,D}$ [28]. The locations of the front stagnation points are also changed at different Knudsen numbers.

The calculating results of the total drag coefficient are shown in Fig. 9. At any outer-inner radii ratio, the drag coefficient increases with increasing the Knudsen number. The geometrical factor becomes insignificant on the drag at $H/R \geq 6$ under continuum flow regime conditions (Fig. 9a), and at $H/R \geq 4$ in free-molecule flow regime. The influence of a ratio of the specific heats γ on drag of a torus is moderate (about 10%) for transition rarefied-flow regimes (Fig. 9b). The drag coefficient is more sensitive to the parameter γ in near-free-molecule flow regimes [20,28].

6. Aerodynamics of toroidal ballute models in dissociating and perfect gas flows

The hypersonic flows of oxygen near a toroidal ballute model [27] have been investigated numerically with the DSMC technique [2,11] under transitional rarefied conditions (Knudsen numbers $Kn_{\infty,D}$ from 0.005 to 1).

The effect of dissociation on chocking of ducted flows has been studied numerically for a

ballute model with varying area ratio H/H_*. The present study confirms the hypothesis [27] that the flow of dissociating gas (oxygen) (Fig. 10a) is not choked at the "designed" toroid [27] with a throat radius H_* = 0.014 m, but the flow of perfect gas (Fig. 10b) is choked at the similar conditions [28]. The following parameters were used in calculations: $Kn_{\infty,D}$ = 0.005, torus radius R = 0.003 m, upstream velocity U_∞ = 5693 m/s, static pressure p_∞ = 1.28 kPa, and temperature T_∞ = 1415 K.

(a)

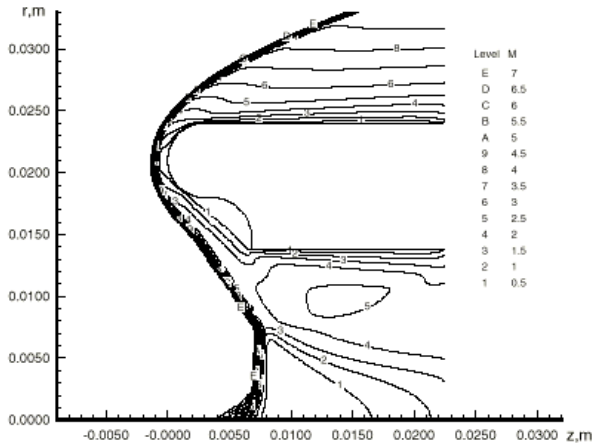

(b)

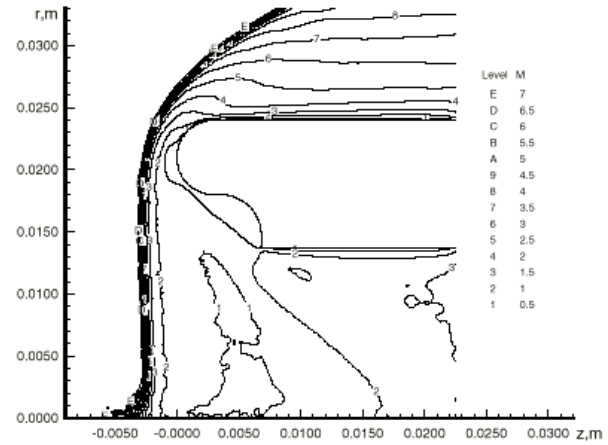

Fig. 10. Mach number contours in oxygen flow about a toroidal ballute model at $Kn_{\infty,D}$ = 0.005: (a) dissociating oxygen flow and (b) perfect-gas oxygen flow.

7. Plate over a plane surface

In the case of a plate over a surface [21], the subsonic area between the plane surfaces becomes much wider than in the case of two side-by-side plates (see Figs 11a-11c). The detached shock wave interacts with the growing boundary layer above the surface. For $Kn_{\infty,L}$ = 0.071 and M_∞ = 10, this effect results in a significant increase (20%) of the repulsive lift force at $2H/L \geq 1$ (see Fig. 12).

(a)

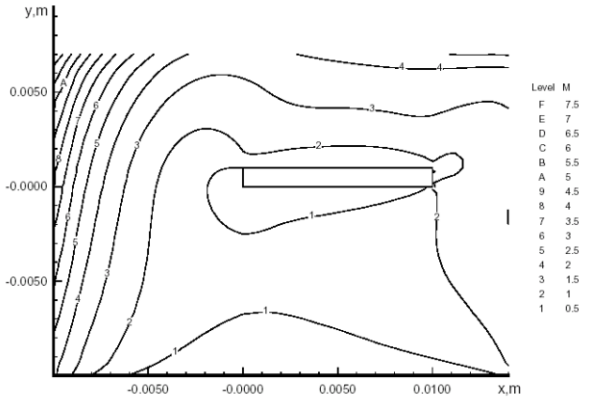

(b)

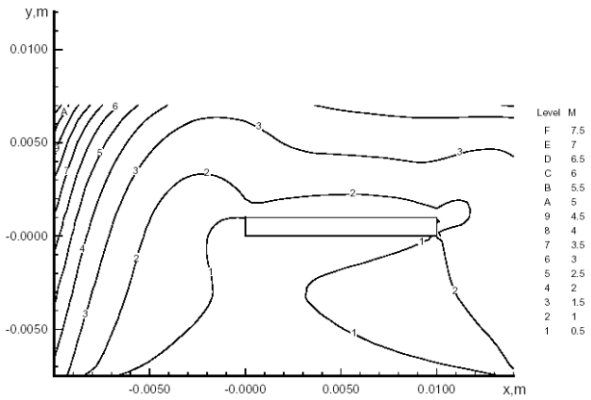

(c)

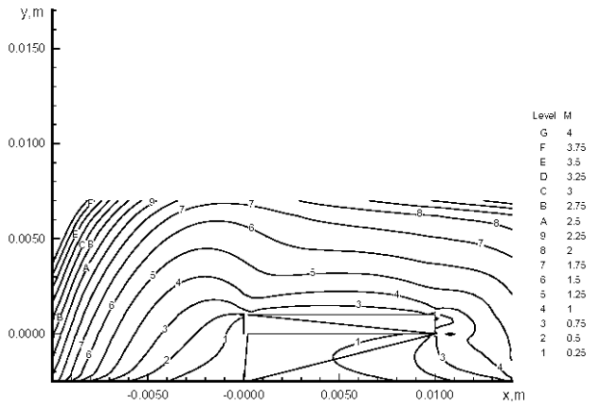

Fig. 11. Mach number contours in argon flow about a plate over a plane surface at $Kn_{\infty,L}$ = 0.07 and various H/L-ratios: (a) H=L, (b) H=0.75L, and (c) H=0.25L.

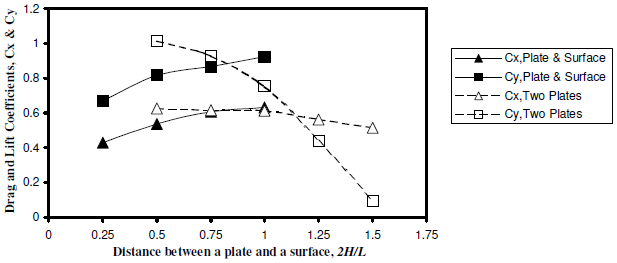

Fig. 12. Total drag and lift coefficients of a plate over a surface vs coefficients of two side-by-side plates.

8. Cylinder over a plane surface

(a)

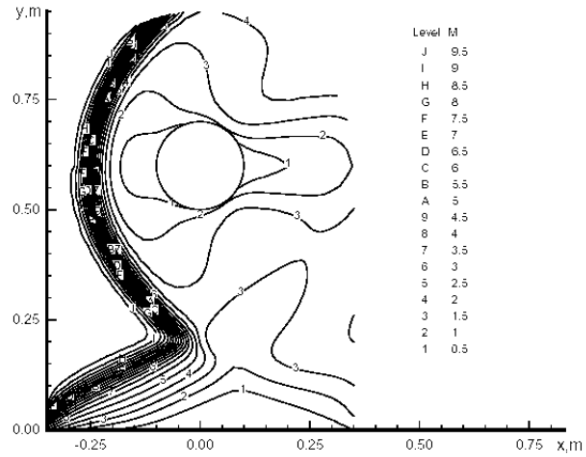

(b)

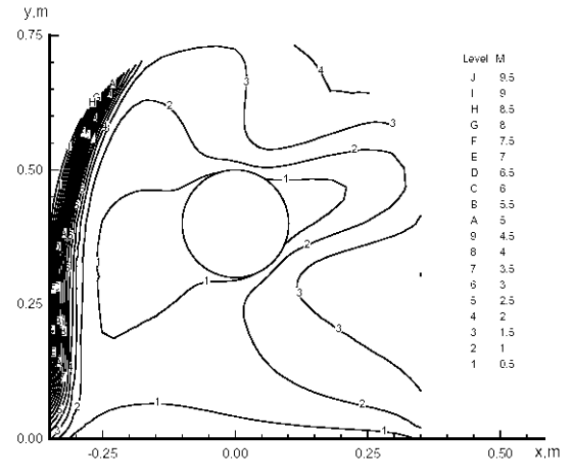

Fig. 13. Mach number contours in argon flow about a cylinder over a plate at $Kn_{\infty,R}$ = 0.1 and various H/R-ratios: (a) $H = 6R$ and (b) $H = 4R$.

The argon flow about a cylinder located over a plane surface has been considered at $Kn_{\infty,L}$ = 0.1 and M_∞ = 10. At a large distance between them, $H \geq 6R$, the interference of the shock waves does not change significantly the symmetrical flow near the cylinder (see Fig. 13a), and the repulsive lift force is negligible [21]. At the smaller ratio parameters, $H/R \leq 4$, the front shock-wave shape becomes normal (see Fig. 13b) and, as a result of interference between the shock wave and the growing boundary layer near the surface, the subsonic area about the cylinder becomes asymmetrical and much wider than in the case of two side-by-side cylinders. The latter effect results in a significant increase (more than 20%) of the repulsive lift force at $H/R \leq 4$.

9. Plate in the wake of a cylindrical wire

(a)

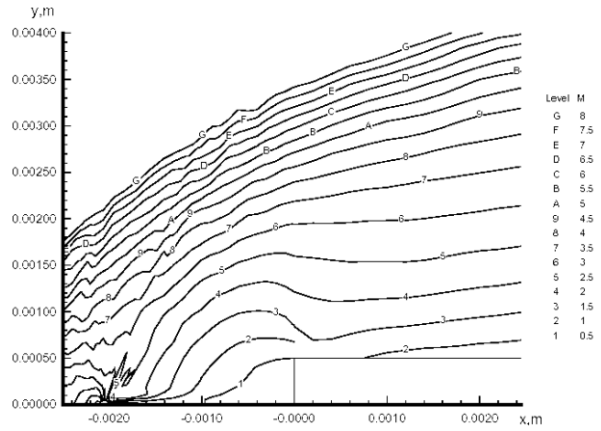

(b)

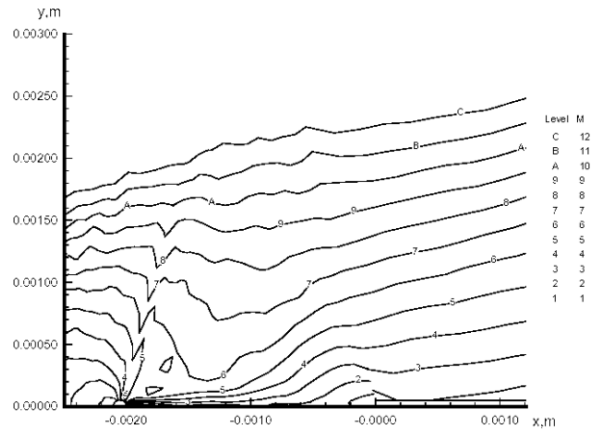

Fig. 14. Mach number contours in nitrogen flow about a plate in the wake of a cylinder at $Kn_{\infty,L}$ = 0.004, t/L = 0.1, Δ/L = 0.2, L = 0.01 m, and various D/t-ratios: (a) D/t = 0.1 and (b) D/t = 1.

In the present analysis, the major regularities in hypersonic rarefied-gas flow about a plate (L = 0.01 m) with a thickness ratio $0.01 \leq t/L \leq 0.1$ located in the wake of a circular cylinder (10^{-4} m $\leq D \leq 10^{-3}$ m) have been studied under the

conditions [13-17, 21] of the strong interaction regime. The analysis of two-dimensional nitrogen flow is made using the DSMC technique [2,11] for rarefied-gas flow regimes at Knudsen number $Kn_{\infty,L}$ = 0.004, Mach number M_∞ = 15, stagnation temperature T_0 = 1100 K, and wall temperature T_w = 295 K.

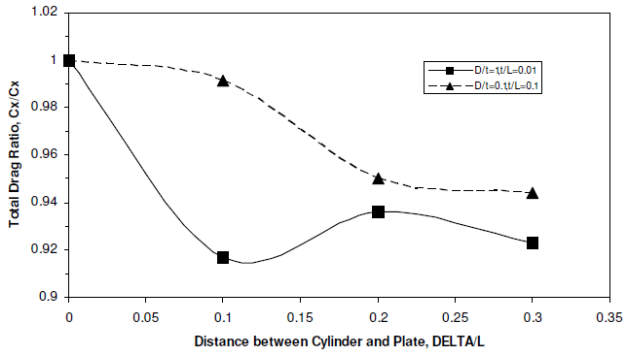

Fig. 15. Effect of the distance between cylinder and plate, Δ, on the total drag of the plate.

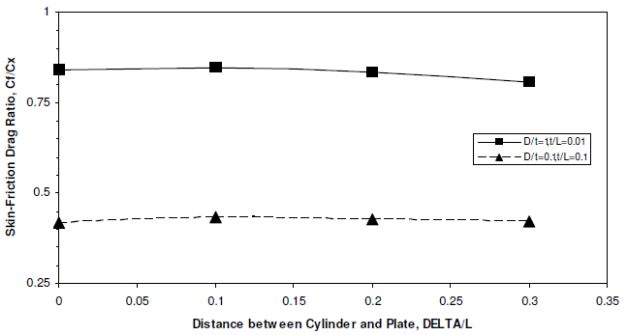

Fig. 16. Effect of the distance between cylinder and plate, Δ, on the skin-friction drag of the plate.

The influence of the geometrical factors of interference between a plate and a cylinder (i.e., the distance between the leading edge of a plate and a rear point of a cylinder, Δ, and the ratio of the cylinder diameter to the plate thickness, D/t) on flowfield characteristics, skin-friction and pressure distributions along the surfaces of the bodies, and on the drag has been studied. The location of the external boundary with the upstream flow conditions varies from 2D to 5D. The wake behind the cylinder interacts with the shock wave near the leading edge of a plate. This interaction results in increasing the size of subsonic zone (see Figs. 14a and 14b) and in redistributing pressure and skin friction along the plate. The flow pattern is different for various D/t-ratios. The induced wake flow in the front area of the plate reduces the strength of the shock wave and results in reducing the plate drag up to 8.3% (see Fig. 15) and friction – up to 5% (see Fig. 16). The maximal reduction of the plate drag is observed at D/t = 1 and Δ/L = 0.1. These findings are in the qualitative agreement with experimental data of Bisch [16].

10. Concluding remarks

The hypersonic rarefied-gas flows about two side-by-side plates and cylinders, a plate and cylinder over a plane surface, and a plate behind a cylinder in argon and nitrogen have been studied using the direct simulation Monte-Carlo technique [29]. The flow pattern and shock-wave shapes are significantly different for small and large geometric ratios. At a value of the geometrical ratio parameter H/L of 0.5, the disturbances interact in the vicinity of the symmetry plane, creating a normal shock wave and a wide subsonic area, which occupies the whole “throat” area between the plates. This phenomenon affects the drag, pressure and skin-friction distributions along the plates, and produces significant repulsive lift force. A non-monotonic dependency of lift, drag and lift-drag ratio versus Knudsen number has been found for different geometric factors. The rarefaction effects on the lift force are significant at all considered values of the geometric factor ($1.25 \geq H/L \geq 0.25$), and they are responsible for non-monotonic dependency of the lift force and lift-drag ratio with the maximum value of 1.7.

The similar effects have been found in the case of hypersonic argon flow about two side-by-side cylinders. At the small ratio parameters, $H/R \leq 3$, the front shock-wave shape becomes normal, a wide subsonic area occupies the whole “throat” area between the cylinders, and the front stagnation points relocate from the cylinder front zone to the throat area. This phenomenon affects the drag, pressure and skin-friction distributions along the cylinders, and produces significant repulsive lift force with the lift-drag ratio of 0.35.

Hypersonic flows about a toroidal balloon and its aerodynamic characteristics have been

investigated in nitrogen, argon, dissociating oxygen, and carbon dioxide at $8R \geq H \geq 2R$ and the Knudsen number $Kn_{\infty,D}$ from 0.005 to 10. The effect of dissociation on chocking of ducted flows has been studied numerically for a ballute model with varying an aspect area ratio, H/H_*. The present study confirms the Lourel's hypothesis [27] that the flow of dissociating oxygen is not choked at the "designed" toroid with a throat radius H_* = 0.014 m, but the flow of perfect gas is choked at the similar conditions.

The subsonic area between the plate and a plane surface becomes much wider than in the case of two side-by-side plates. This effect results in the significant increase (more than 20%) in the repulsive lift force at $2H/L \geq 1$.

In the case of a blunt plate located in the wake of a cylindrical wire, the induced wake flow in front of the plate reduces the strength of the shock wave and results in reducing the plate drag up to 8.3%. The considered examples demonstrate the importance of studying the interference effects in applied hypersonic aerodynamics.

Acknowledgments

The author would like to express gratitude to Dr. G. A. Bird for the opportunity of using the DS2G computer program, Dr. J. N. Moss for valuable discussions of the DSMC technique, and to I. Lourel for providing experimental data received at the X2 expansion tube of the University of Queensland, Brisbane, Australia.

References

[1] Koppenwallner G, Legge H. Drag of bodies in rarefied hypersonic flow. In: *Thermophysical Aspects of Reentry Flows*, edited by Moss JN, Scott CD, Vol. 103, Progress in Astronautics and Aeronautics. New York, NY: AIAA; 1994, pp. 44-59.

[2] Bird GA. *Molecular gas dynamics and the direct simulation of gas flows*. Oxford, England, UK: Oxford University Press; 1994, pp. 340-377.

[3] Gusev VN, Erofeev AI, Klimova TV, Perepukhov VA, Riabov VV, Tolstykh AI. Theoretical and experimental studies of flow over bodies of simple shape by a hypersonic stream of rarefied gas. Trudy TsAGI 1977; 1855:3-43 (in Russian).

[4] Riabov VV. Comparative analysis of hypersonic rarefied gas flows near simple-shape bodies. J Spacecraft and Rockets 1998; 35(4):424-433.

[5] Gorelov SL, Erofeev AI. Qualitative features of a rarefied gas flow about simple shape bodies. In: *Rarefied Gas Dynamics*, edited by Belotserkovskii OM, Kogan MN, Kutateladze SS, Rebrov AK. 13th Intern. Symposium Proceedings, Vol. 1. New York, NY: Plenum Press; 1985, pp. 515-521.

[6] Lengrand JC, Allège J, Chpoun A, Raffin M. Rarefied hypersonic flow over a sharp flat plate: numerical and experimental results. In: *Rarefied Gas Dynamics: Space Science and Engineering*, edited by Shizdal BD, Weaver DP, Vol. 160, Progress in Astronautics and Aeronautics. New York, NY: AIAA; 1994, pp. 276-284.

[7] Riabov VV. Numerical study of hypersonic rarefied-gas flows about a torus. J Spacecraft and Rockets 1999; 36(2):293-296.

[8] Coudeville H, Trepaud P, Brun EA. Drag measurements in slip and transition flow. In: *Rarefied Gas Dynamics*, edited by de Leeuw JH. 4th Intern. Symposium Proceedings, Vol. 1. New York, NY: Academic Press; 1965, pp. 444-466.

[9] Mavriplis C, Ahn JC, Goulard R. Heat transfer and flowfields in short microchannels using direct simulation Monte Carlo. J Thermophys Heat Transfer 1997; 11(3):489-496.

[10] Oh CK, Oran ES, Sinkovits RS. Computations of high-speed, high Knudsen number microchannel flows. J Thermophys Heat Transfer 1997; 11(3):497-505.

[11] Bird GA. The DS2G program user's guide, version 3.2. Killara, Australia: G.A.B. Consulting Pty; 1999, pp. 1-56.

[12] Blevins RD. *Applied fluid dynamics handbook*. Malabar, FL: Krieger Publishing; 1992, pp. 318-333.

[13] Hayes W D, Probstein RF. *Hypersonic flow theory*. New York, NY: Academic Press; 1959, pp. 35-67.

[14] Oguchi H. The sharp-leading-edge problem in hypersonic flow. In: *Rarefied Gas Dynamics*, edited by Talbot L. 2nd Intern. Symposium Proceedings. New York, NY: Academic Press; 1961, pp. 501-524.

[15] Allègre J, Bisch C. Angle of attack and leading edge effects on the flow about a flat plate at Mach number 18. AIAA J 1968; 6(5): 848-852.

[16] Bisch C. Drag reduction of a sharp flat plate in a rarefied hypersonic flow. In: *Rarefied Gas Dynamics*, edited by Potter JL. 10th Intern. Symposium Proceedings, Vol. 1 Washington, DC: AIAA; 1976, pp. 361-377.

[17] Yegorov IV, Yegorova MV, Ivanov DV, Riabov VV. Numerical study of hypersonic viscous flow about plates located behind a cylinder. AIAA Paper 97-2573. Washington, DC: AIAA; 1997, 1-10.

[18] Riabov VV. Aerodynamics of two side-by-side plates in hypersonic rarefied-gas flows. J Spacecraft and Rockets 2002; 39(6):910-916.

[19] Riabov VV. Interference between two side-by-side cylinders in hypersonic rarefied-gas flows. AIAA Paper 2002-3297. Washington, DC: AIAA; 2002, 1-9.

[20] Kogan MN. *Rarefied gas dynamics*. New York, NY: Plenum Press; 1969, pp. 345-390.

[21] Riabov VV. Aerodynamics of two interfering simple-shape bodies in hypersonic rarefied-gas flows. In: *Rarefied Gas Dynamics*, edited by Ketsdever AD, Muntz EP. 23rd Intern. Symposium Proceedings. Melville, NY: American Institute of Physics; Vol. 663, 2003, pp. 489-496.

[22] Hall JL, Le AK. Aerocapture trajectories for spacecraft with large, towed ballutes. AAS/AIAA Space Flight Mechanics Meeting, Paper AAS 01-235. Washington, DC: AIAA; 2001, 1-10.

[23] Gnoffo PA, Anderson BP. Computational analysis of towed ballute interactions. AIAA Paper 2002-2997. Washington, DC: AIAA; 2002, 1-9.

[24] Moss JN. DSMC simulations of ballute aerothermodynamics under hypersonic rarefied conditions. AIAA Paper 2005-4949. Washington, DC: AIAA; 2005, 1-15.

[25] McIntyre TJ, Lourel I., Eichman TN, Morgan RG, Jacobs PA, Bishop AI. Experimental expansion tube study of the flow over a toroidal ballute. J Spacecraft and Rockets 2004; 41(5):716-725.

[26] Lourel I., Eichmann TN, Isbister S, McIntyre TJ, Houwing AFP, Morgan RG. Experimental and numerical studies of flows about a toroidal ballute. Proceedings of the 23rd International Symposium on Shock Waves, Paper 5038. Fort Worth, TX, July 22-27, 2001; pp. 1-7.

[27] Lourel I, Morgan RG. The effect of dissociation on chocking of ducted flows. AIAA Paper 2002-2894. Washington, DC: AIAA; 2002, 1-11.

[28] Riabov VV. Numerical study of hypersonic rarefied-gas flows about a toroidal ballute. In: *Rarefied Gas Dynamics*, edited by Ivanov MS, Rebrov AK. 25th Intern. Symposium Proceedings. Novosibirsk, Russian Academy of Sciences; 2007, pp. 765-770.

[29] Riabov VV. Numerical study of interference between simple-shape bodies in hypersonic flows. Computers and Structures 2009; 87 (11-12):651-663.

Contact Author Email Address

The contact author email address:
vriabov@rivier.edu

Copyright Statement